

# PREPARATION AND CHARACTERIZATION OF THIN-FILM COMPOSITE REVERSE OSMOSIS MEMBRANE ON A NOVEL AMINOSILANE-MODIFIED POLYVINYL CHLORIDE SUPPORT

Shahram T. Iranizadeh<sup>1,2</sup>, M. Pourafshari Chenar<sup>1,2\*</sup>,  
Mahdieh N. Mahboub<sup>3</sup> and Hamed A. Namaghi<sup>4</sup>

<sup>1</sup> Ferdowsi University of Mashhad, Faculty of Engineering, Chemical Engineering Department, Mashhad, Iran.  
E-mail: shahram\_irani99@yahoo.com; pourafshari@um.ac.ir, ORCID: 0000-0001-7173-4421

<sup>2</sup> Ferdowsi University of Mashhad, Faculty of Engineering, Research Center of Membrane Processes and Membrane, Mashhad, Iran.

<sup>3</sup> University of Gonabad, Department of Chemical Engineering, Gonabad, Iran. E-mail: namvar@gonabad.ac.ir

<sup>4</sup> Semnan University, Faculty of Chemical, Petroleum and Gas Engineering, Semnan, Iran. E-mail: ha.azizi@semnan.ac.ir

(Submitted: September 18, 2017 ; Revised: February 22, 2018 ; Accepted: March 26, 2018)

**Abstract** - Herein, the influence of pure and modified polyvinyl chloride (PVC) support layers on the performance of thin-film composite (TFC) membranes was investigated in water desalination. Accordingly, the PVC support was modified using (3-Aminopropyl) triethoxysilane (APTES) through bulk modification. The supports were synthesized at different doses of APTES (0-6 wt%) and characterized with various analytical techniques. The results showed that APTES affected considerably both the morphology and surface properties of the support layer. Afterwards, the polyamide (PA) layer was formed via an identical interfacial polymerization (IP). The separation experiments showed that modification of the support improved the performance of the TFC membranes, which stems from the improvement in the degree of cross-linking of the PVC structure. At an appropriate condition, permeate fluxes were 0.89 L.m<sup>-2</sup>.h<sup>-1</sup>.bar<sup>-1</sup> and 2.70 L.m<sup>-2</sup>.h<sup>-1</sup>.bar<sup>-1</sup> for TFC membranes with pure and modified PVC support layers, respectively. Interestingly, there were no significant changes in salt rejection of the prepared membranes.

**Keywords:** Thin film composite membrane; Support layer modification; PVC; Cross-linking; APTES.

## INTRODUCTION

To meet increased global demand, treatment of saline water resources plays a crucial role for the management of fresh water supply. Over the past few decades, reverse osmosis (RO) was the most promising separation process in terms of water desalination and wastewater treatment (Kim and Lee, 2011; Elimelech and Phillip, 2011). Although both asymmetric and TFC membranes are developed in large scale, TFC ones, including a selective PA layer on top of a porous support, are the preferable structure for RO membranes due to their excellent chemical stability, high rejection

and water flux (Elimelech and Phillip, 2011; Geise et al., 2010; Park et al., 2017). Additionally, in the case of TFC membrane, the structure and properties of each layer can be tailored independently. This ability provides an opportunity to optimize the performance of TFC membranes by the enhancement of the physicochemical properties of each layer separately (Ghosh and Hoek, 2009). Thus, the related studies to improve the performance and durability of RO membrane are divided into two categories (i.e., support modification and PA modification). In the case of PA layer modification, there are several studies which focused on the upgrading of PA structure through

\* Corresponding authors: Mahdi P. Chenar - E-mail: pourafshari@um.ac.ir

altering the monomers or IP conditions (Kim et al., 2005; Yong et al., 2006; Ghosh et al., 2008; Wei et al., 2010; Kong et al., 2010; Xie et al., 2012). However, the morphology and surface physiochemical properties of the support layer can affect the structure of the PA layer, water permeation rate and also salt rejection of TFC membrane. Therefore, the optimization of the support layer should also be considered.

Polysulfone (PSf) and polyethersulfone (PES) are the most widely used polymers for the preparation of the support layer of PA-TFC RO membranes (Mohan and Kullová, 2013; Seman et al., 2010; Son et al., 2015; Azizi Namaghi et al., 2015). Although these polymers show good thermal stability and tolerance to a wide range of pH values, they have relatively hydrophobic surfaces and low chemical stability in aromatic hydrocarbons (Kim et al., 2009; Ahmad et al., 2013). Recently, some studies have been carried out to overcome the above mentioned limitations. Accordingly, the support layer of TFC membranes was modified via inserting modifiers in the polymer matrix (Ghosh and Hoek, 2009; Son et al., 2015; Mahdavi and Hosseinzadeh, 2015; Sotto et al., 2012; Arena et al., 2011; Yan et al., 2016). Furthermore, altering the polymer material was suggested for preparation of the support layer in the literature, which will be summarized as follows. Kim et al. (2009) applied a polyvinylidene fluoride (PVDF) support layer to prepare PA-TFC membranes. They used low temperature plasma to improve the hydrophilicity of commercial PVDF membrane. Their results showed that plasma treatment of PVDF membrane increased the surface hydrophilicity, which is required for the preparation of TFC membrane through the IP method. The experimental results also indicated that PA/PVDF membrane had higher water flux and salt rejection than PA/PSf membrane. Kim and Soo Kim (2006) studied the effect of low temperature plasma treatment of polypropylene (PP) and PSf support membranes on the performance of TFC-RO membranes. Accordingly, hydrophilic additives, including acrylic acid, acrylonitrile, allylamine, ethylenediamine and *n*-propylamine were also used to increase the hydrophilicity of the support membranes. They reported that plasma treatment substantially improved the performance of PA/PP composite membranes. Their results also showed that plasma treatment of the support not only enhanced the adhesion properties between the active layer and support, but also improved the chlorine resistance of the TFC membrane. Poly (phthalazinone ether sulfone ketone) (PPESK) was also used by Wei et al. (2005) as the thermally stable support material for the preparation of TFC membranes. They claimed that the thermal stability of PA/PPESK membranes is higher than that of PA/PSf membranes. At 1.2 MPa pressure and 20°C,

a fully aromatic PA/PPESK TFC membrane rejected 2000 ppm NaCl solution by 98% and water flux was 10.1 L.m<sup>-2</sup>.h<sup>-1</sup>. By increasing the feed temperature from 20°C to 80°C, water flux increased more than two-fold without reduction of salt rejection. Akbari et al. (2015) focused on the preparation of TFC membranes via IP of polyethyleneimine and trimesoyl chloride on polyacrylonitrile (PAN) as the support layer. They positively charged the surface of the prepared TFC membranes through cross-linking of the PA layer with *p*-xylylenedichloride (XDC) and glutaraldehyde (GA). The results illustrated that salt rejection followed the sequence of CaCl<sub>2</sub>>NaCl>Na<sub>2</sub>SO<sub>4</sub>.

As reviewed, regarding the required properties of the support layer, different polymers can be used during fabrication of the support membrane. Among the available polymers, polyvinyl chloride (PVC) is an appropriate candidate for preparation of the support layer due to its high mechanical strength, low cost, high chemical resistance and high lifetime, even after chemical cleaning or chlorine disinfection process (Liu et al., 2013; Liu et al., 2013; Zhang et al., 2009; Huang et al., 2009). Although PVC has considerably lower cost than many polymers, lower hydrophilicity and water flux make it less desirable than traditional polymers like PSf to apply as UF membranes (Yu et al., 2015). Accordingly, modification of the physicochemical properties of PVC membranes should be concerned to develop its potential application in the preparation of TFC membranes (Zhao et al., 2016). Bulk modification, which incorporates inorganic or organic additives into the polymer matrix through solution blending, is widely used to enhance the properties of the polymeric membranes. In the case of PVC membranes, both organic and inorganic additives such as amphiphilic copolymer (Pluronic F 127) (Liu et al., 2013), graphene oxide (Zhao et al., 2016), SiO<sub>2</sub> (Yu et al., 2014), TiO<sub>2</sub> (Behboudi et al., 2016), ZnO (Rabiee et al., 2015) and PEG (Abadi Farahani et al., 2015) were applied to modify the membrane properties. Since inorganic nanoparticles show low interaction with polymer chains, it is required to functionalize nanoparticles with agents like aminosilanes, surfactants or acids. As reported by Siddique et al. (2014), aminosilanes as organosilicone precursor generate an inorganic-organosiloxane network (Si–O–Si). Therefore, aminosilane agents such as APTES can be added into the polymer matrix to make a mixed matrix membrane (MMM). In addition, it can be used as cross-linker for polymer chains like PVC owing to their functional groups.

To the best of the authors' knowledge, there is no report on the modification of PVC membrane using aminosilane agents. Also, PVC has not been used as the support layer of flat sheet TFC membranes so far. Accordingly, this work focused on the preparation of

mixed matrix PVC membranes for application as the support layer of TFC-RO membranes. For this purpose, different amounts of APTES were incorporated into the PVC matrix. The effect of additive dosage on the morphology and surface properties of as-prepared support membranes was investigated by using Fourier transform infrared (FTIR) spectroscopy, scanning electron microscopy (SEM), energy-dispersive X-ray spectroscopy (EDS), atomic force microscopy (AFM), and contact angle analyses. Moreover, the PA layer was formed on the as-prepared supports via an identical IP process of *m*-phenylenediamine (MPD) and trimesoyl chloride (TMC) monomers. Finally, the performance of the resultant TFC membranes was investigated through desalination of a 2000 ppm NaCl aqueous solution and it was compared with the performance of PA/PSf membrane.

## MATERIALS AND METHODS

### Chemicals

The polyester (PET) webbing used for new TFC membrane preparation was obtained from old RO spiral wound modules. In this regard, the permeate spacer (usually its composition is polyester) of old RO modules was used as the new polyester after washing with DI water and drying in the oven. PVC (K68) polymer was obtained from Bandar Imam Petrochemical Co. (Iran) without any additive. The PSf (Ultrason 6010) with the average molecular weight of 45000–55000 g/mol was provided by BASF Co. (Germany). TMC monomer was purchased from Sigma Aldrich. MPD monomer, *N*-methyl-2-pyrrolidone (NMP) and *n*-hexane solvents were supplied by Merck. In order to determine the separation performance of synthesized TFC membrane, 2 g of sodium chloride (NaCl, crystals from Merck) were dissolved in 1000 mL of deionized (DI) water obtained from a 5 stage water purification system (Aqua-spring).

### Preparation of PA/Modified PVC Membrane

Support membranes were prepared via the non-solvent induced phase separation (NIPS) method. Accordingly, a certain amount of polymer (PVC or PSf) was dissolved in NMP and a homogeneous solution was obtained after stirring. Then, different doses (0–6 wt%) of APTES were added into the polymeric solution and it was stirred until a homogeneous solution was obtained. It should be noted that the PVC solution was stirred at 50 °C. The composition of casting solutions is summarized in Table 1.

All samples were nominated according to the composition of polymer and APTES. As can be seen, composition of total dissolved materials was 16 wt% for most of polymer solutions.

To synthesize the PA layer, the IP technique was conducted. To do this, as-prepared mixed matrix

**Table 1.** Composition of the support membrane casting solutions and sample names.

TFC code	Support code	Polymer (wt%)	APTES (wt%)	NMP (wt%)
TFC16-A0	PVC16-A0	16	0	84
TFC13-A3	PVC13-A3	13	3	84
TFC12-A4	PVC12-A4	12	4	84
TFC10-A6	PVC10-A6	10	6	84
TFC12-A0	PVC12-A0	12	0	88
TFC	PSU16-A0	16	-	84

support layers were immersed in an aqueous solution of MPD (2%w/v) for 2 minutes. The surface of saturated membranes was firmly pressed with a soft rubber roller to remove excess solution. The membranes saturated with MPD solution were subsequently exposed to the organic solution of TMC (0.1%w/v) for 20 seconds to react with the MPD and form the PA selective layer. Finally, the membranes were post-treated and dried in the oven for 10 minutes at 60 °C. The resultant TFC membranes were nominated according to the applied support layer (Table 1).

### Membrane Characterization

#### FTIR Test

To investigate the presence of the Si–O–Si bond that corresponds to the APTES and the reaction between polymer chains and inorganic additive, FTIR analysis was conducted using an Avatar 370 Nicolet Spectrometer. FTIR spectra of pure and mixed matrix PVC membranes were obtained in the range of 4000 to 400 cm<sup>-1</sup>.

#### SEM and EDS Tests

Surface and cross-sectional structures of as-prepared supports and TFC membranes were studied through SEM images obtained by scanning electron microscopy (SEM, LEO1450VP, Zeiss, Germany) at 20 kV. The presence of APTES in the polymer matrix was probed using EDS detector.

#### AFM analysis

To evaluate surface roughness of the as-prepared membranes, AFM analysis (full plus series 0101/A, Ara, Iran) was conducted. Small pieces of each sample (1 cm × 1 cm) were prepared and scanned in a size of 10 μm by 10 μm. The membrane surface roughness was expressed in terms of the average roughness ( $R_a$ ) and the root mean square of the Z data ( $R_q$ ).

#### Contact Angle Measurement

To study the effect of additive on the hydrophilicity of as-prepared support layers, the surface contact angle of membranes was measured. For this purpose, measurements were performed based on the sessile drop method via a contact angle measuring instrument (OCA15 plus, 196 Data physics, Germany). The

reported results are the average contact angle of DI water droplets at three different locations on each sample.

### TFC Membrane Performance

The performance of TFC membranes was investigated through desalination of an aqueous solution (2000 ppm concentration of NaCl) at an operating pressure of 7 bar and room temperature. Experiments were carried out using a lab-scale system containing a cross-flow cell. The effective filtration area of the membrane in the module is 10.18 cm<sup>2</sup>. Details of this experimental setup were described previously (Azizi Namaghi et al., 2015). Membrane performance including water flux,  $J$  (L.m<sup>-2</sup>.h<sup>-1</sup>(LMH)), and salt rejection,  $R$ , were calculated using the following equations:

$$J = \frac{1}{S} \cdot \frac{dV}{dt} \quad (1)$$

$$R = \left( 1 - \frac{C_p}{C_f} \right) \times 100 \quad (2)$$

where  $V$  (L) is the volumetric flow rate of permeate;  $S$  (m<sup>2</sup>) is the effective membrane area;  $t$  (h) is the sampling time;  $C_p$  (mg/L) is the concentration of NaCl in the permeate flow; and  $C_f$  (mg/L) is the concentration of NaCl in the feed solution. After 150 minutes of operation, the permeate flux nearly approached the steady state condition and the permeate samples were collected to measure water permeate flux and salt rejection. The TDS values of the feed and permeate were measured using an electrical conductivity meter from Extech EC-400 (USA). These analytical procedures and the results obtained from them are described in the next section.

## RESULTS AND DISCUSSION

### FTIR Analysis

The effect of aminosilane on the structure of PVC membrane was investigated via FTIR analysis. In view of this, FTIR spectra of pure PVC (PVC16-A0) and aminosilane-modified PVC (PVC12-A4) membranes are illustrated in Figure 1. The monomer units in PVC are for the most part joined head-to-tail. The chemical structure could therefore be written as (-CH<sub>2</sub>CHCl-). Accordingly, the characteristic bands of pure PVC can be categorized into three regions. The first region is the C-Cl stretching in the range of 600-700 cm<sup>-1</sup>. The second one is C-C stretching in the range from 900 to 1200 cm<sup>-1</sup>. The third one is 1250-2970 cm<sup>-1</sup> in PVC (numerous C-H modes). Furthermore, in the

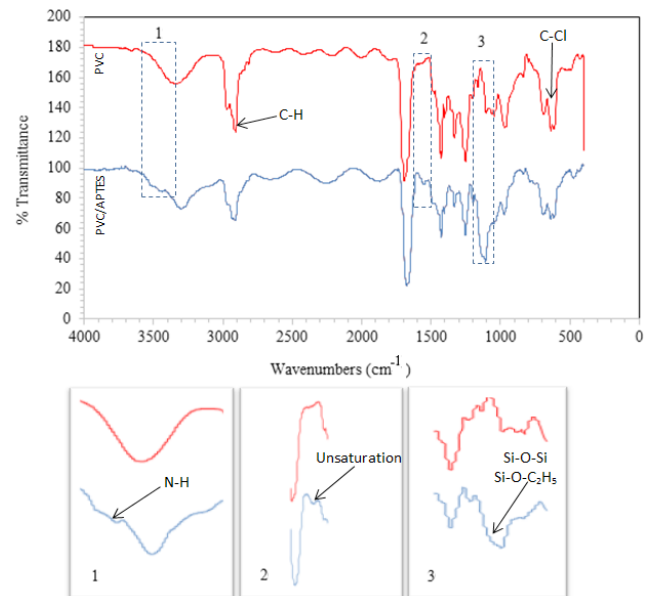


**Figure 1.** FTIR spectra of pure PVC and PVC/APTES.

pure PVC spectrum, the bands at 1331, 1253, and 950 cm<sup>-1</sup> are assigned to CH<sub>2</sub> deformation, CH rocking and CH wagging of PVC, respectively (Kayyrapu et al., 2016).

For pure PVC, the chlorine atoms were orientated randomly along the chain. Since the chlorine atoms stick out from the chain at random, and because of their large size and high electronegativity, it is difficult for the chains to lie close together. Consequently, PVC is mainly amorphous with only small areas of crystallinity. Amorphous polymers are more flexible than crystalline ones, because the forces of attraction between the chains tend to be weaker. So, APTES was used to create a new bond with the PVC polymeric membrane based on the reaction schematized in Figure 2. In the case of modified PVC membranes, a new band is observed at 3440 cm<sup>-1</sup> which is related

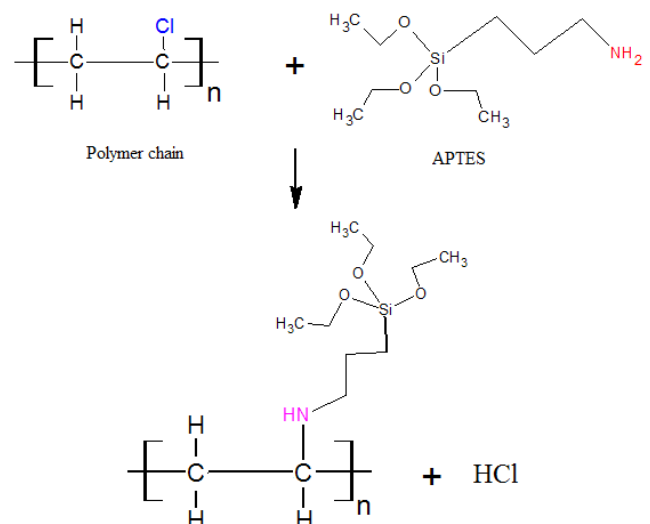


**Figure 2.** Schematic reaction of PVC and APTES.



to the N–H bond of the aminosilane functional group. The band at  $1107\text{ cm}^{-1}$  is attributed to the ethoxy group of APTES. The bands in the range of  $1000\text{--}1200\text{ cm}^{-1}$  corresponded to  $\text{Si-O-CH}_2\text{CH}_3$  which overlapped with the band of the  $\text{Si-O-Si}$  bond. In addition, the intensity of the characteristic bands of PVC decreased for modified PVC because of reduction in the PVC amount. The band at  $1600\text{ cm}^{-1}$  is related to the substitution reaction which displaced chlorine atoms with nitrogen atoms. The above mentioned reaction

apparently cross-linked the polymer chains using the aminosilane agent (APTES) (Rodriguez-Fernandez and Gilbert, 1997).

### SEM Analysis

#### Structure of Support Membrane

The morphology of pure and modified PVC were probed via SEM analysis. Surface structure views of pure PVC and mixed matrix PVC/APTES membranes are presented in Figure 3. As can be observed, the

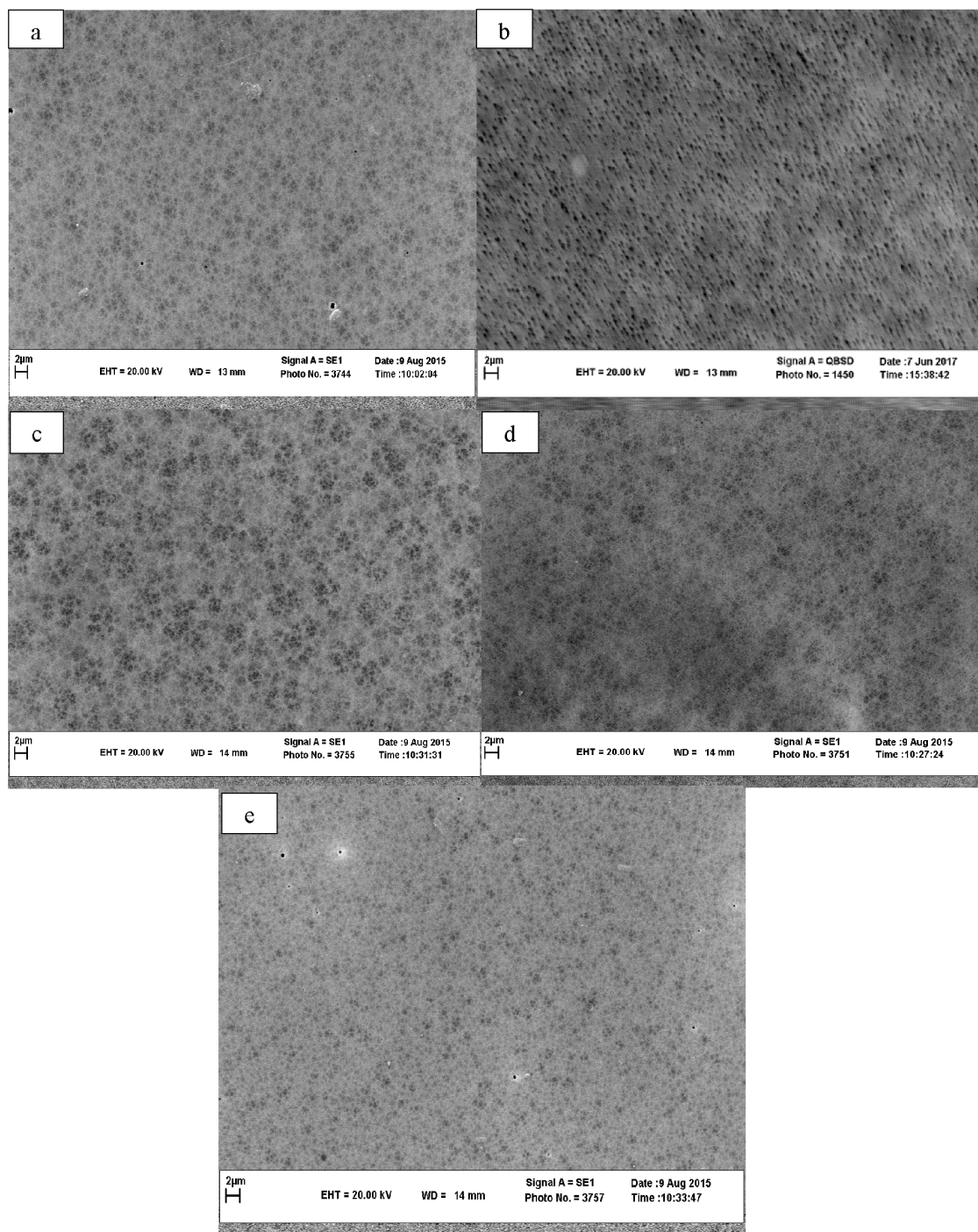


**Figure 3.** Surface images of support membranes, a) PVC12-A0, b) PVC10-A6, c) PVC12-A4, d) PVC13-A3 and e) PVC16-A0.

surface pore size of as-prepared membranes depended on the concentration of PVC and APTES in the casting solution. Also, for pure PVC membranes, surface pore sizes decrease upon increasing the concentration of polymer from 12 to 16 wt%. In fact, increasing the polymer content leads to a reduction of the solvent-nonsolvent exchange rate during the demixing process. As a result, delayed demixing will occur and a more compact structure will be created.

Surface SEM images of modified PVC membranes were compared with that of pure PVC membrane to investigate the effect of additive dosage on morphology of the PVC membranes (Figure 3). As can be seen, the surface structure of the support membranes becomes dense in the sequence of PVC16-A0 > PVC13-A3 >

PVC12-A4 > PVC10-A6, respectively. This trend is due to the decreasing polymer content when the APTES dosage increases. Comparison of surface images of PVC12-A0 and PVC12-A4 shows that, at the same polymer concentration, the presence of APTES leads to the formation of smaller pores on the surface of the support layer. As described in the FTIR section, APTES was used to create a new bond with the PVC polymeric membranes based on a chemical reaction. This new bond can improve the interconnectivity between the pores on the surface of the membrane.

Cross-sectional views of pure and modified PVC membranes with different doses of APTES are presented in Figure 4. All of the membranes synthesized with NMP exhibited a top approximately dense skin

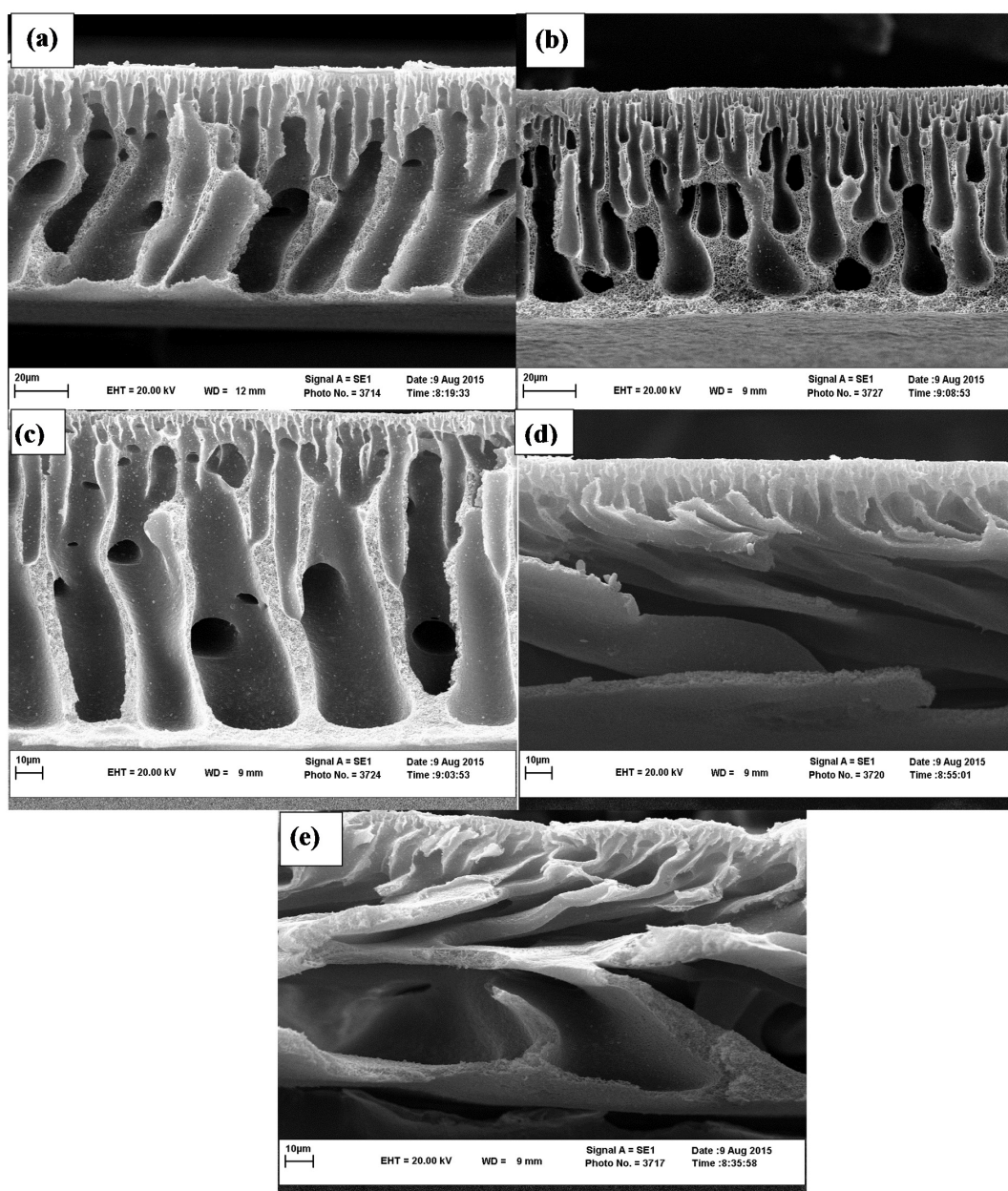


**Figure 4.** Cross-sectional images of the support membranes, a) PVC12-A0, b) PVC16-A0, c) PVC13-A3, d) PVC12-A4 and e) PVC10-A6.



layer, a porous sub-layer and fully developed finger-like pores along with several macrovoids at the bottom as a consequence of the strong affinity and miscibility between solvent (NMP) and non-solvent (DI water) in the coagulation bath (Peyravi et al., 2012). The presence of finger-like pores is related to the rate of solvent-nonsolvent exchange, which leads to the instantaneous demixing. Also, the mode of the demixing process (delayed demixing or instantaneous demixing) has a direct relationship with the thermodynamic instability and the interaction diffusivities (kinetic behavior) between components in the system during precipitation of the casting solution (Mohammadi and Saljoughi, 2009). The cross-sectional views of PVC12-A0 and PVC16-A0 were compared to study the effect of polymer concentration. Obviously, the cross-section of PVC12-A0 depicts larger pores and a less dense structure when compared with that of PVC16-A0. Furthermore, the wall thickness increased upon increasing polymer concentration. In general, the polymer rich phase becomes denser upon increasing the polymer concentration in the casting solution, which tends to reduce transport rates and thereby produces a delayed demixing. The combination of these factors could contribute to a thicker top layer, lower porosity and hinders void growth (Deng et al., 2014; Strathmann and Kock, 1977).

In the case of MMMs, with the increment of the APTES content, the finger-like voids became larger. As shown in Figure 4(b) to 4(e), when the APTES dosage increases from 0 to 6%, the common finger-like structure converts to an irregular porous structure. It seems that the presence of APTES in the polymer matrix based on the demixing pathway and mechanism of membrane formation has a dual effect on the support membrane morphology. On the one hand, by incorporation of APTES into the polymer matrix, cross-linking of polymer chains takes place via a silanol bond (Rodriguez-Fernandez and Gilbert, 1997). In this case, APTES acts as a cross-linker which leads to the suppression of macrovoids. On the other hand, the hydrophilic nature of APTES assists solvent molecule transport through the polymer chains, and consequently, the solvent-nonsolvent exchange rate increases (hinders delayed demixing). In this case, nuclei of voids can be rapidly developed and large microvoids may be formed (Strathmann and Kock, 1977). All in all, the final structure depends on the superiority of instantaneous or delayed demixing and comes from the presence of APTES in the polymer casting solution.

In addition, with the increment of the APTES content, the polymer dosage decreases from 16 to 10 % (Table 1). The decline of the polymer dosage leads to the formation of a less viscous casting solution. Therefore, the diffusional exchange rate between solvent (NMP) and non-solvent (water) during the

precipitation process in the coagulation bath were slowed down (hinders instantaneous demixing).

### Structure of TFC Membrane

The structure and intrinsic properties of the support layer directly affect the structure and performance of TFC membranes. Accordingly, the surface morphologies of TFC membranes, prepared via the same IP conditions on pure PVC, PVC/APTES and pure PSf support layers, are presented in Figure 5. The variation in the surface morphology of TFC membrane compared to the PVC support layer demonstrated that a PA layer was formed over all supports. For PA membranes, "ridge and valley" is the dominant structure, which is characteristic of MPD/TMC. Anyhow, the PA structure of TFC12-A0 is less extended than that of TFC16-A0. Undeniably, increasing the polymer content of the support layer leads to the formation of smaller surface pores (as shown in Figs. 3 and 4). These small pores dominate MPD diffusion through the pores and, as a consequence, a more cross-linked polymer structure will be formed. Thus, a thicker and denser PA layer may be generated and the morphology alters from the "ridge and valley" to a "nodular" structure (Kong et al., 2016). In the case of TFC membranes containing PVC/APTES support layers, both "ridge and valley" and "nodular" structures can be observed. By increasing the APTES dosage up to 6 wt%, the PA structure changed from "ridge and valley" to "nodular" form. Altering the top layer morphology is definitely due to the change of the support layer. In this case, the pore size and the physicochemical properties of the surface influence the synthesis mechanism of the PA layer. As mentioned before, large and irregular microvoids of the support membrane provide an effortless path for MPD molecules to diffuse through pores. Thus, TMC reacts with MPD within the pores and a thinner and less dense polyamide selective layer will be formed. Larger pores permit more MPD diffusion and less cross-linked polyamide chains (Singh et al., 2006). Additionally, the  $\text{NH}_2$  groups of APTES enhance the support membrane hydrophilicity, which limits diffusion of MPD in the support layer (Ghosh and Hoek, 2009). In this case, some TMC may diffuse into the pores and react with  $\text{NH}_2$  groups of the support layer and, as a result, less TMC participates in the IP reaction. Thus, less dense polyamide will be created within the pores of PVC/APTES membranes compared with that of the pure PVC support layer. In summary, more APTES content leads to smaller surface pores of the support layer, a dense and thicker PA layer and finally a rougher surface of the resultant TFC membrane. Comparing the PA surface structure of TFC membranes demonstrates that TFC (with pure PSf support), TFC12-A4 and also TFC13-A3 have similar surface structure. Therefore, it is expected that these three membranes will have similar performance.

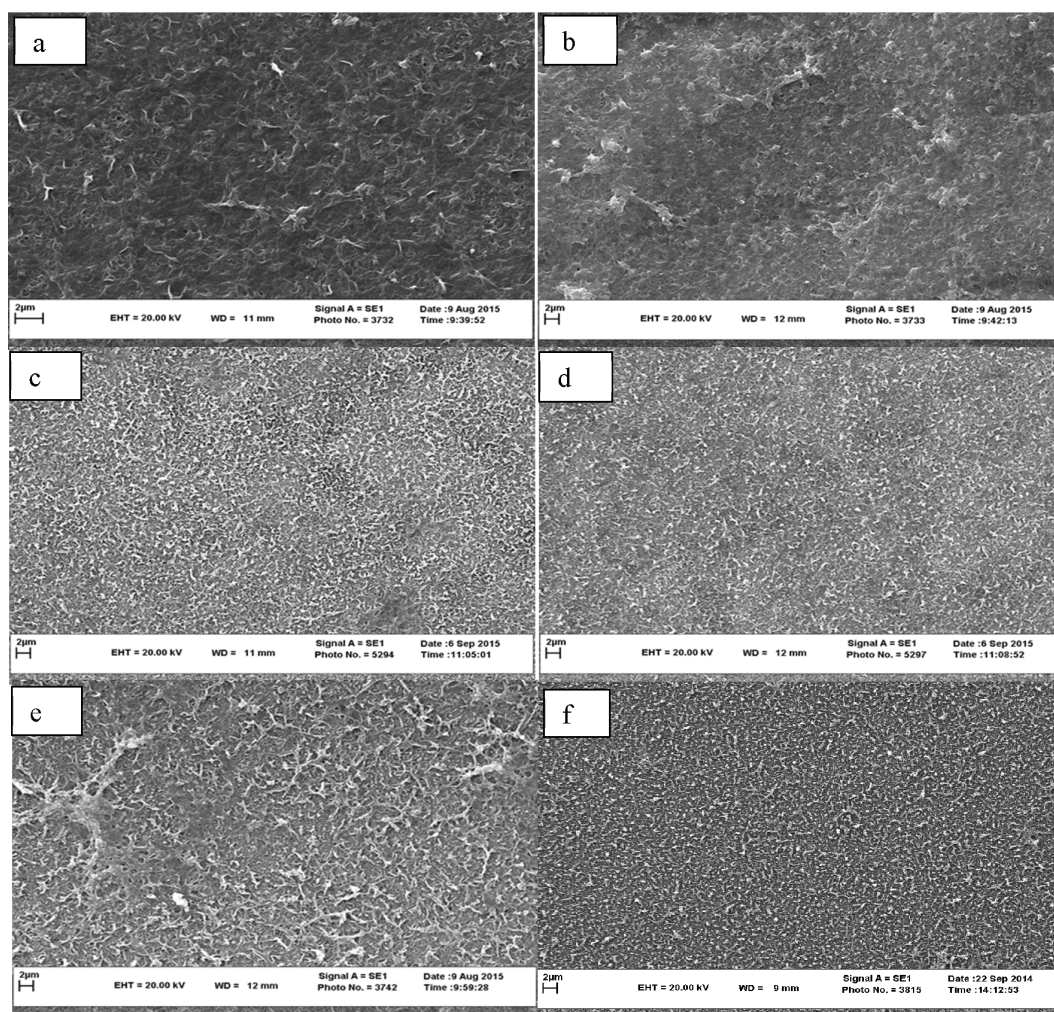


**Figure 5.** Surface images of TFC membranes, a) TFC12-A0, b) TFC10-A6, c) TFC12-A4, d) TFC13-A3, e) TFC16-A0 and f) TFC.

### EDS Analysis of the Support Layer

The presence of the aminosilane group in the polymer matrix is confirmed by EDS analysis. Figure 6 depicts the spectra at specific parts of the surface and cross-section of the PVC/APTES support layer. The results show the peak, which is attributed to Si, for both cases. This reveals that APTES is well-dispersed in the polymer matrix. In addition, the peaks of Cl, C and oxygen are detected. These elements belong to the PVC chains. Besides, an Au peak is present due to the sputtering layer of gold on the membrane samples. Since polymers are generally insulators, membrane samples have to be sputtered under vacuum with a thin layer of gold to produce electrical conductivity, eliminate surface charging, and also minimize sample damage caused by the electron beam.

### AFM Analysis

Figure 7 illustrates the AFM images of modified PVC, neat PSf, PA/modified PVC and PA/PSf membranes. In addition, the surface roughness parameters including; the average roughness,  $R_a$ , and

the root mean square of the Z data,  $R_q$ , are reported for the above-mentioned samples (Table 2). As can be seen for support membranes, the modified PVC support membrane has lower roughness than a traditional PSf support layer. Additionally, the results show that a TFC membrane with modified PVC as support layer is smoother than a TFC membrane with PSf as support. This observation is in agreement with SEM micrographs. According to the conceptual model of the PA formation mechanism, a rough surface of the membrane results in higher retention of hydrated ions and water flux (Ghosh and Hoek, 2009; Madaeni, 2004).

### Contact Angle Measurements

The average contact angle values of pure and MMMs are presented in Table 3. As can be seen, incorporation of a small amount of APTES in the polymer matrix increases hydrophilicity of PVC/APTES membranes compared with pure PVC. Interestingly, the contact angle value increased  $\sim 10^\circ$  (from  $70.73^\circ$  to  $80.16^\circ$ ) when the APTES dosage increased from 3 to 6 wt%. The



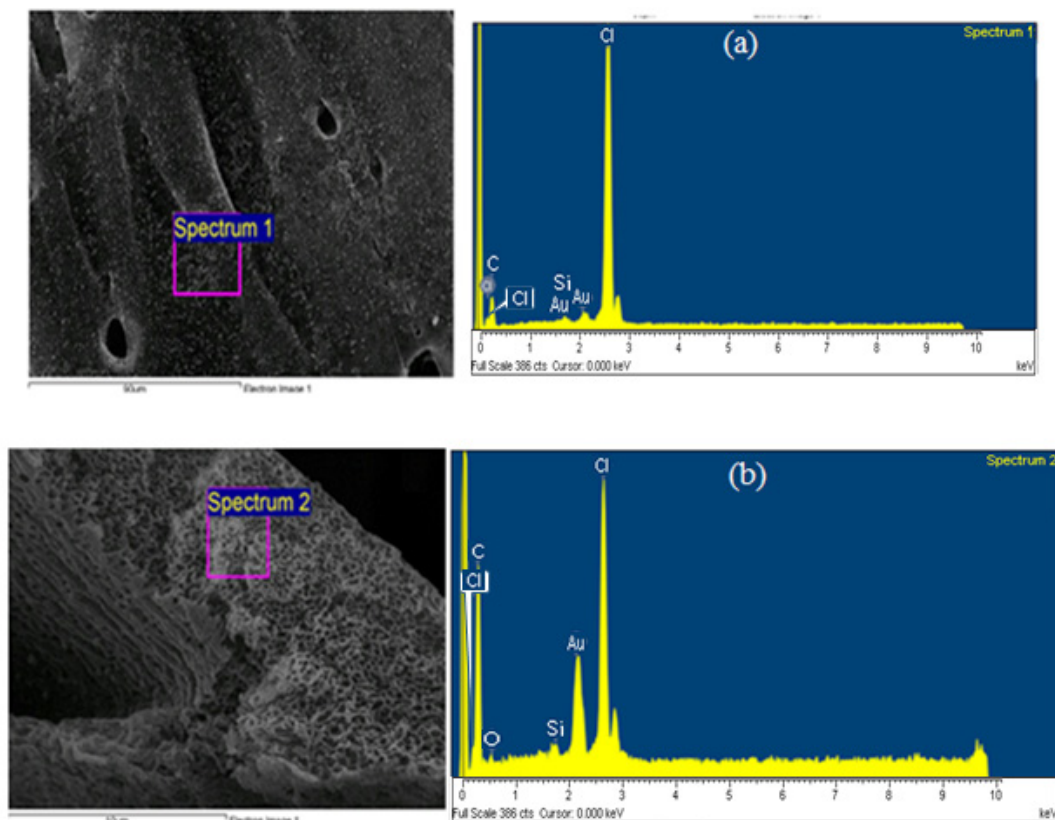


**Figure 6.** EDS spectrum of the PVC/APTES support layer (a) surface and (b) cross-section.

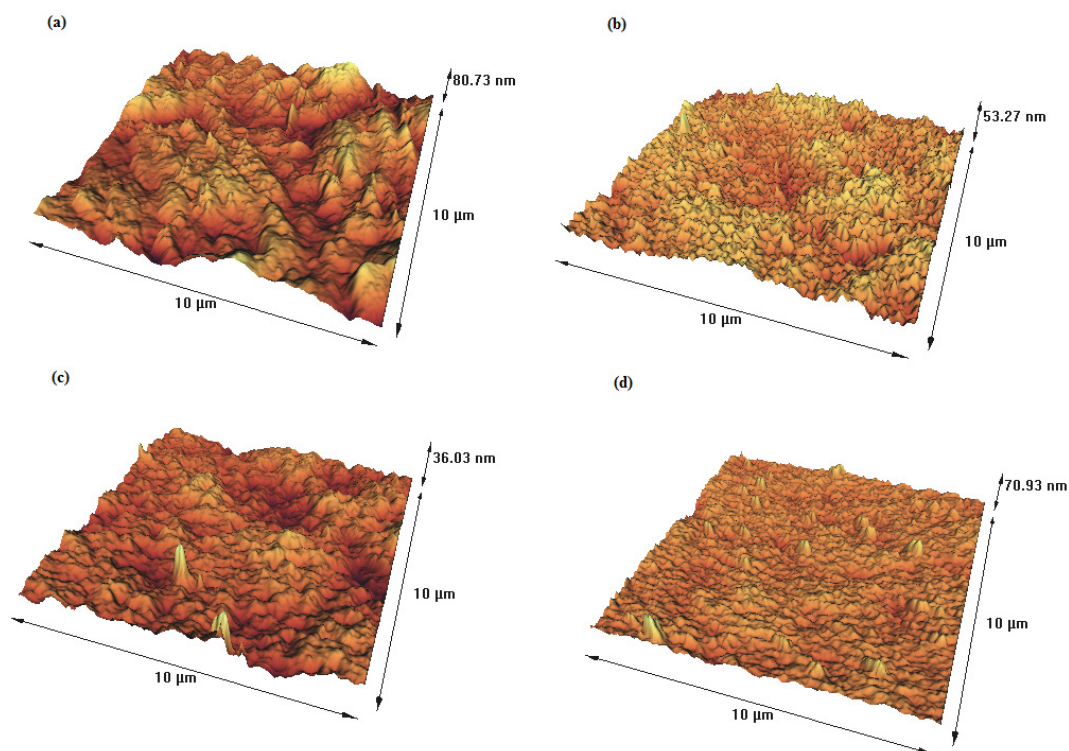


**Figure 7.** Three dimensional AFM images of a) pure PSf support, b) modified PVC support, c) PA/PSf membrane, d) PA/modified PVC membrane.

chemical structure of APTES and surface roughness of as-prepared TFC membranes can elucidate this

behavior. APTES contains aliphatic hydrocarbon and amine groups, which show hydrophobic and

**Table 2.** Surface roughness parameters of the support and TFC membranes.

Membrane code	R <sub>a</sub> (nm)	R <sub>q</sub> (nm)
PSf16-A0	1.802±0.268	12.997±3.735
PVC12-A4	0.899±0.151	6.48±0.672
TFC	0.791±0.019	4.833±0.842
TFC12-A4	0.725±0.026	4.076±1.065

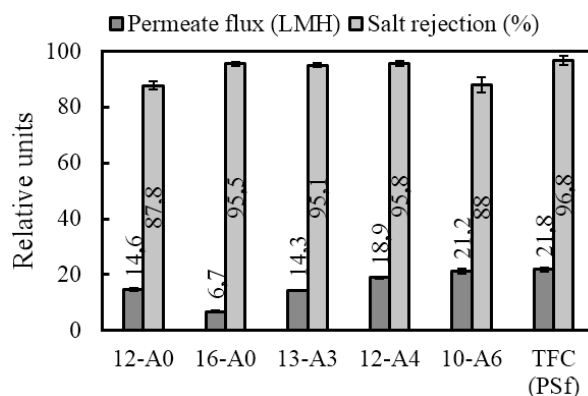
hydrophilic properties, respectively (Arkles, 2006). During cross-linking of the polymer matrix, N–H and Si–O–Si bonds will be created and aliphatic groups hindered in the polymer matrix. The above mentioned bonds have polar nature and hydrophilic properties. Thus, the cross-linking degree of the polymer matrix can also affect hydrophilicity. On the other hand, some part of the additive seems not to participate in the cross-linking reaction at high dosage of APTES. In such circumstance, hydrophobic ethoxy groups of the membrane matrix will be more than Si–O–Si bonds and the final hydrophilicity of as-prepared membranes decreases in comparison with a low dosage of APTES embedded polymer matrix. On the other hand, as can be observed by surface micrographs, the PA layer of the TFC-A3 membrane is smoother than that of TFC-A6. Since surface roughness is inversely related to the contact angle, thus by increasing surface roughness, the contact angle value is reduced.

### Performance of TFC Membranes

The separation performance of as-prepared TFC membranes was studied through desalination of synthetic salt water. The results of performance parameters, permeate flux and salt rejection are plotted in Figure 8. It can be observed that, by increasing APTES dosage and reducing polymer concentration, the permeate flux increased from 6.7 L.m<sup>-2</sup>.h<sup>-1</sup> to 21.2 L.m<sup>-2</sup>.h<sup>-1</sup> for TFC16-A0 and TFC10-A6, respectively. As observed in SEM and FTIR analyses, the cross-linking extent of the polymer chain of the membrane increased upon increment of the APTES dosage. Also, the degree of cross-linking of APTES with PVC affected the pore structure (pore size and porosity) and physicochemical properties of the support layer. Finally, the performance of the TFC membranes is influenced by morphological and physicochemical properties of both selective (PA) and non-selective (support) layers. A possible explanation for this might be that the relatively hydrophobic substrates produced characteristically thicker, rougher and more permeable PA layers. One would expect thicker films to be less dense, and thus more permeable (Ghosh and Hoek, 2009). An increase of the cross-linking

extent decreases water flux, while hydrophilicity and larger pore size increase water flux (McCutcheon and Elimelech, 2008). Additionally, the mentioned effects lead to the formation of a less compact and thinner PA selective layer. Thus, it is expected that permeate flux increases and salt rejection decreases for TFC16-A0 to TFC10-A6, respectively. However, at low dosage of APTES (3 and 4 wt%), there is no visible reduction in salt rejection due to a suitable cross-linking degree of PA chains with low thickness of the layer. In addition, at the same PVC content, TFC12-A4 shows higher flux than TFC12-A0. These relationships may be partly explained by the pore size and porosity of the support layer which are directly affected by polymer concentration (Figs. 4a and 4c) and decrease with increasing polymer concentration. Tight pore structure of the support would limit the diffusion of MPD aqueous solution deep into the pores, resulting in formation of a thicker PA layer and greater surface roughness (Azizi Namaghi et al., 2015; Misdan et al., 2013). Furthermore, the increase of water flux could be attributed to a higher effective area of PA (as evidence in Figure 5) when a more porous support layer was applied (Deng et al., 2014).

In the case of salt rejection, TFC membranes show a different trend when APTES is inserted into the support layer. From Figure 8, it is found that, at low content of APTES (3 and 4 wt%), there is no observable changes in salt rejection of TFC13-A3 and TFC12-A4 compared with that of TFC16-A0, while for TFC10-A6 a severe reduction in salt rejection can be observed. In the case of same polymer content, salt rejection increases from 87.8 % to 95.8% for TFC12-A0 and TFC12-A4, respectively. The reasons leading to a decrease and increase in the permeate flux with altering polymer concentration and APTES content in the support, which have been elucidated in

**Figure 8.** Experimentally determined separation performance of TFC membranes.**Table 3.** Contact angle values of as-prepared support membranes.

	PVC16-A0	PVC13-A3	PVC12-A4	PVC10-A6	PSf
CA (°)	84±1.01	70.73±1.18	75.49±0.85	80.16±0.83	76.46±1.3



preceding paragraphs, can account for increasing and decreasing the rejection rate.

All in all, TFC membranes which were prepared using a modified PVC support layer with low content of APTES have enhanced performance parameters than pure PVC TFC membrane. Consequently, a low amount of APTES has a positive effect on the permeate flux and salt rejection of as-prepared TFC membranes. In reviewing the literature, no data was found on the association between PVC/APTES MMMs and TFC membrane performance. But, a strong relationship between support and TFC membrane performance has been reported in prior studies. In one well-known report, Ghosh and Hoek (2009) explained that the variance in the surface chemistry and physical structure of PSf substrates produced widely varying PA layer morphology, interfacial properties, and separation performance. They reported that a more hydrophobic and rough PSf support produced a PA layer with higher water permeability, while a support with large pores produced a PA layer with higher salt permeability.

The results of PA/PSf membranes based on a given PA synthesis condition are also presented in Figure 8. The results implied that PA/PVC membranes cannot effectively compete with PA/PSf membranes without modification. However, it seems that aminosilane modification of the PVC support layer enhances the performance of PA/modified PVC membranes and makes their performance comparable with PA/PSf membranes for the same synthesis conditions of the PA layer. For this purpose, TFC12-A4 was considered as the PA/modified PVC membrane due to its better performance and similar hydrophilicity and PA surface structure (Figs. 5c and 5f).

The decline in permeate flux across the membrane after a specific period of time is one of the most important properties of the membrane system. Also, internal fouling by irreversible physical compaction still remains a serious concern for RO membranes. Although surface deposits of solutes on the PA surface are easily removed by chemical cleaning, membrane compaction is irreversible (Pendergast, 2010). Accordingly, Figure 9 illustrates the permeate flux values versus time for as-prepared TFC membranes. The results showed that the permeate flux slightly declined as a function of time in a similar trend for all TFC membranes. This means that the support layer has no individual effect on membrane fouling through the desalination process. Also, the flux reduction trend can be attributed to concentration polarization, compaction and also accumulation, precipitation and absorption of retained solutes (salt) on the membrane surface. Furthermore, it is obvious from Figure 9 that all mixed matrix TFC membranes produced higher flux than pure PVC TFC membranes. The single exception to this trend was TFC13-A3; however, the

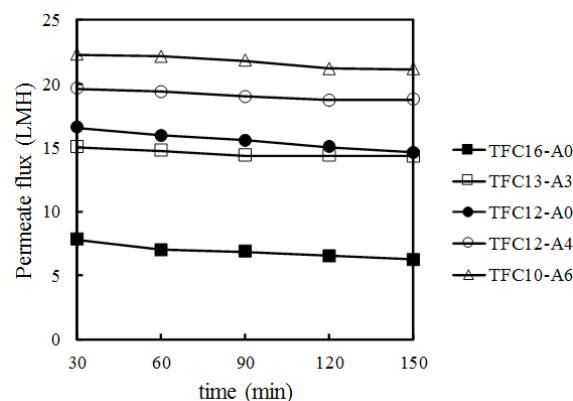


**Figure 9.** Permeate flux of as-prepared TFC membranes as a function of time at 7 bar.

permeate flux of TFC13-A3 seems to be equalized with the permeate flux of TFC12-A0 at the end of the experiment. The permeate flux decline rates are higher for pure PVC TFC membranes compared to mixed matrix ones. Permeate flux decline rates decrease in the order of TFC16-A0 > TFC12-A0 > TFC10-A6 > TFC13-A3 > TFC12-A4. Under the assumption of the same concentration polarization and accumulation, precipitation and absorption of retained solutes on the surface of the membrane, the flux decline rates can be attributed only to the membrane compaction. It is postulated that mixed matrix TFC membranes show a lower flux decline as a consequence of high mechanical strength. In fact, APTES creates a new bond with the PVC polymeric membrane based on a substitution reaction. This new bond improves the interconnectivity between the pores and improves the mechanical strength. Similar behavior was observed by Namvar et al. (2013). They reported that the mechanical and thermal stability of a polyetherimide (PEI) support were improved with incorporation of amino-functionalized nanosilica in the polymer matrix.

## CONCLUSION

This research was undertaken to develop a novel PVC/APTES MMM and evaluate its performance as the support layer of TFC-RO membranes. Modified support membranes were characterized via FTIR, SEM, EDS, AFM and contact angle analyses. According to the results, FTIR spectra revealed that the aminosilane functional group had been chemically attached and cross-linked with the chloromethylene group (CHCl) of PVC chains. In addition, addition of small amount of APTES up to a certain level improved the support porosity evidenced by cross-section SEM analysis. Also, the support membrane hydrophilicity, porosity, as well as surface pore size effectively influenced the TFC membrane permeability. Building upon the results noted above, we support the idea that

the separation performance and interfacial properties of TFC-RO membranes strongly depend on the properties of the support layer such as material, pore structure, pore size, porosity, surface roughness and hydrophilicity. Overall, it is concluded that the MMM of TFC12-A4 had the best performance parameters for the desalination process. Further investigation and experimentation with PVC and other novel substitutional polymers is highly recommended.

## REFERENCES

- Ahmad, A., Abdulkarim, A., Ooi, B., Ismail, S., Recent development in additives modifications of polyethersulfone membrane for flux enhancement. *Chem. Eng. J.*, 223, 246-267 (2013). <https://doi.org/10.1016/j.cej.2013.02.130>
- Akbari, A., Fakharshakeri, Z., MojallaliRostami, S., A novel positively charged membrane based on polyamide thin-film composite made by cross-linking for nanofiltration. *Water Sci. Technol.*, 73, 776-789 (2015). <https://doi.org/10.2166/wst.2015.538>
- Arena, J., McCloskey, B., Freeman, B., McCutcheon, J., Surface modification of thin film composite membrane support layers with polydopamine: Enabling use of reverse osmosis membranes in pressure retarded osmosis. *J. Membr. Sci.*, 375 (1-2), 55-62 (2011). <https://doi.org/10.1016/j.memsci.2011.01.060>
- Arkles, B., Hydrophobicity, hydrophilicity and silanes. *Paint Coatings Ind.*, 22 (10), 114-135 (2006).
- AziziNamaghi, H., HaghighiAsl, A., and PourafshariChenar, M., Identification and optimization of key parameters in preparation of thin film composite membrane for water desalination using multi-step statistical method. *J. Ind. Eng. Chem.*, 31, 61-73 (2015). <https://doi.org/10.1016/j.jiec.2015.06.008>
- Behboudi, A., Jafarzadeh, Y., Yegani, R., Preparation and characterization of TiO<sub>2</sub> embedded PVC ultrafiltration membranes. *Chem. Eng. Res. Des.*, 114, 96-107 (2016). <https://doi.org/10.1016/j.cherd.2016.07.027>
- DavoodAbadiFarahani, M.H., Rabiee, H., Vatanpour, V., Borghei, S.M., Fouling reduction of emulsion polyvinylchloride ultrafiltration membranes blended by PEG: the effect of additive concentration and coagulation bath temperature. *Desalin. Water Treat.*, 57 (26), 11931-11944 (2015). <https://doi.org/10.1080/19443994.2015.1048739>
- Deng, B., Ding, C., Yin, J., Effects of polysulfone (PSf) support layer on the performance of thin-film composite (TFC) membranes. *J. Chem. Proc. Eng.*, 1, 1-8 (2014). <https://doi.org/10.17303/jce.2014.102>
- Elimelech, M., Phillip, W., The future of seawater desalination: energy, technology, and the environment. *Science*, 333 (6043), 712-717 (2011). <https://doi.org/10.1126/science.1200488>
- Geise, G., Lee, H., Miller, D., Freeman, B., McGrath, J., Paul, D., Water purification by membranes: the role of polymer science. *J. Polym. Sci. Part B: Polym. Phys.*, 48 (15), 1685-1718 (2010). <https://doi.org/10.1002/polb.22037>
- Ghosh, A., Hoek, E., Impacts of support membrane structure and chemistry on polyamide-polysulfone interfacial composite membranes. *J. Membr. Sci.*, 336 (1-2), 140-148 (2009). <https://doi.org/10.1016/j.memsci.2009.03.024>
- Ghosh, A., Jeong, B., Huang, X., Hoek, E., Impacts of reaction and curing conditions on polyamide composite reverse osmosis membrane properties. *J. Membr. Sci.*, 311 (1-2), 34-45 (2008). <https://doi.org/10.1016/j.memsci.2007.11.038>
- Huang, H., Schwab, K. and Jacangelo, J., Pretreatment for low pressure membranes in water treatment: A review. *Environ. Sci. Technol.*, 43 (9), 3011-3019 (2009). <https://doi.org/10.1021/es802473r>
- Kayyarapu, B., Kumar Y.M., Mohommad, H., Neeruganti O.G., Chekuri, R. Structural, thermal and optical properties of pure and Mn<sup>2+</sup> doped poly(vinyl chloride) films. *Mat. Res.*, 19 (5), 1167-1175 (2016). <https://doi.org/10.1590/1980-5373-MR-2016-0239>
- Kim, D., Lee, B., Pilot study analysis of three different processes in drinking water treatment. *Environ. Eng. Res.*, 16(4), 237-242 (2011). <https://doi.org/10.4491/eer.2011.16.4.237>
- Kim, E., Kim, Y., Yu, Q., Deng, B., Preparation and characterization of polyamide thin-film composite (TFC) membranes on plasma-modified polyvinylidene fluoride (PVDF). *J. Membr. Sci.*, 344(1-2), 71-81 (2009). <https://doi.org/10.1016/j.memsci.2009.07.036>
- Kim, H., Kim, S., Plasma treatment of polypropylene and polysulfone supports for thin film composite reverse osmosis membrane. *J. Membr. Sci.*, 286 (1-2), 193-201 (2006). <https://doi.org/10.1016/j.memsci.2006.09.037>
- Kim, S., Kwak, S., Suzuki, T., Positron annihilation spectroscopic evidence to demonstrate the flux-enhancement mechanism in morphology-controlled thin-film-composite (TFC) membrane. *Environ. Sci. Technol.*, 39 (6), 1764-1770 (2005). <https://doi.org/10.1021/es049453k>
- Kong, C., Kanezashi, M., Yamamoto, T., Shintani, T., Tsuru, T., Controlled synthesis of high performance polyamide membrane with thin dense layer for water desalination. *J. Membr. Sci.*, 362 (1-2), 76-80 (2010). <https://doi.org/10.1016/j.memsci.2010.06.022>



- Kong, X., Zhou, M.Y., Lin, C.E., Wang, J., Zhao, B., Wei, X.Z., Zhu, B.K., Polyamide/PVC based composite hollow fiber nanofiltration membranes: Effect of substrate on properties and performance. *J. Membr. Sci.*, 505, 231-240 (2016). <https://doi.org/10.1016/j.memsci.2016.01.028>
- Liu, B., Chen, C., Zhang, W., Crittenden, J., Chen, Y., Low-cost antifouling PVC ultrafiltration membrane fabrication with Pluronic F 127: Effect of additives on properties and performance. *Desalination*, 307, 26-33 (2012). <https://doi.org/10.1016/j.desal.2012.07.036>
- Madaeni, S.S., Effect of surface roughness on retention of reverse osmosis membranes. *J. Porous Mat.*, 11 (4), 255-263 (2004). <https://doi.org/10.1023/B:JOPO.0000046352.14487.6f>
- Mahdavi, H., Hosseinzadeh, M., A suitable polyethersulfone membrane support for polyamide thin film composite nanofiltration membrane: preparation and characterization. *J. Iran Chem. Soc.*, 12 (8), 1347-1356 (2015). <https://doi.org/10.1007/s13738-015-0600-5>
- McCutcheon, J.R., Elimelech, M., Influence of membrane support layer hydrophobicity on water flux in osmotically driven membrane processes. *J. Membr. Sci.*, 318 (1), 458-466 (2008). <https://doi.org/10.1016/j.memsci.2008.03.021>
- Misdan, N., Lau, W.J., Ismail, A.F., Matsuura, T., Formation of thin film composite nanofiltration membrane: effect of polysulfone substrate characteristics. *Desalination*, 329, 9-18 (2013). <https://doi.org/10.1016/j.desal.2013.08.021>
- Mohammadi, T., Saljoughi, E., Effect of production conditions on morphology and permeability of asymmetric cellulose acetate membranes. *Desalination*, 243 (1-3), 1-7 (2009). <https://doi.org/10.1016/j.desal.2008.04.010>
- Mohan, D., Kullová, L., A study on the relationship between preparation condition and properties/performance of polyamide TFC membrane by IR, DSC, TGA, and SEM techniques. *Desalin. Water Treat.*, 51 (1-3), 586-596 (2013). <https://doi.org/10.1080/19443994.2012.693655>
- Namvar-Mahboub, M., Pakizeh, M., Development of a novel thin film composite membrane by interfacial polymerization on polyetherimide/modified SiO<sub>2</sub> support for organic solvent nanofiltration. *Sep. Purif. Technol.*, 119, 35-45 (2013). <https://doi.org/10.1016/j.seppur.2013.09.003>
- Park, S., Choi, W., Nam, S., Hong, S., Lee, J., Lee, J., Fabrication of polyamide thin film composite reverse osmosis membranes via support-free interfacial polymerization. *J. Membr. Sci.*, 526, 52-59 (2017). <https://doi.org/10.1016/j.memsci.2016.12.027>
- Pendergast, M.T.M., Nygaard, J.M., Ghosh, A.K., Hoek, E.M., Using nanocomposite materials technology to understand and control reverse osmosis membrane compaction. *Desalination*, 261 (3), 255-263 (2010). <https://doi.org/10.1016/j.desal.2010.06.008>
- Peyravi, M., Rahimpour, A., Jahanshahi, M., Thin film composite membranes with modified polysulfone supports for organic solvent nanofiltration. *J. Membr. Sci.*, 423, 225-237 (2012). <https://doi.org/10.1016/j.memsci.2012.08.019>
- Rabiee, H., Vatanpour, V., Farahani, M., Zarrabi, H., Improvement in flux and antifouling properties of PVC ultrafiltration membranes by incorporation of zinc oxide (ZnO) nanoparticles. *Sep. Purif. Technol.*, 156, 299-310 (2015). <https://doi.org/10.1016/j.seppur.2015.10.015>
- Rodriguez-Fernandez, O.S., Gilbert, M., Aminosilane grafting of plasticized poly(vinyl chloride) II. Grafting and crosslinking reactions. *J. Appl. Polym. Sci.*, 66 (11), 2121-2128 (1997). [https://doi.org/10.1002/\(SICI\)1097-4628\(19971219\)66:11%3C2121::AID-APP8%3E3.0.CO;2-J](https://doi.org/10.1002/(SICI)1097-4628(19971219)66:11%3C2121::AID-APP8%3E3.0.CO;2-J)
- Seman, M., Khayet, M., Hilal, N., Nanofiltration thin-film composite polyester polyethersulfone-based membranes prepared by interfacial polymerization. *J. Membr. Sci.*, 348 (1-2), 109-116 (2010). <https://doi.org/10.1016/j.memsci.2009.10.047>
- Siddique, H., Rundquist, E., Bhole, Y., Peeva, L., Livingston, A., Mixed matrix membranes for organic solvent nanofiltration. *J. Membr. Sci.*, 452, 354-366 (2014). <https://doi.org/10.1016/j.memsci.2013.10.012>
- Singh, P.S., Joshi, S.V., Trivedi, J.J., Devmurari, C.V., Rao, A.P., Ghosh, P.K., Probing the structural variations of thin film composite RO membranes obtained by coating polyamide over polysulfone membranes of different pore dimensions. *J. Membr. Sci.*, 278 (1), 19-25 (2006). <https://doi.org/10.1016/j.memsci.2005.10.039>
- Son, M., Choi, H., Liu, L., Celik, E., Park, H., Choi, H., Efficacy of carbon nanotube positioning in the polyethersulfone support layer on the performance of thin-film composite membrane for desalination. *Chem. Eng. J.*, 266, 376-384 (2015). <https://doi.org/10.1016/j.cej.2014.12.108>
- Sotto, A., Rashed, A., Zhang, R., Martínez, A., Braken, L., Luis, P., Van der Bruggen, B., Improved membrane structures for seawater desalination by studying the influence of sublayers. *Desalination*, 287, 317-325 (2012). <https://doi.org/10.1016/j.desal.2011.09.024>
- Strathmann, H., Kock, K., The formation mechanism of phase inversion membranes. *Desalination*, 21 (3), 241-255 (1977). [https://doi.org/10.1016/S0011-9164\(00\)88244-2](https://doi.org/10.1016/S0011-9164(00)88244-2)

- Wei, J., Jian, X., Wu, C., Zhang, S., Yan, C., Influence of polymer structure on thermal stability of composite membranes. *J. Membr. Sci.*, 256, 116-121 (2005). <https://doi.org/10.1016/j.memsci.2005.02.012>
- Wei, X., Wang, Z., Chen, J., Wang, J., Wang, S., A novel method of surface modification on thin-film-composite reverse osmosis membrane by grafting hydantoin derivative. *J. Membr. Sci.*, 346 (1), 152-162 (2010). <https://doi.org/10.1016/j.memsci.2009.09.032>
- Xie, W., Geise, G., Freeman, B., Lee, H., Byun, G., McGrath, J., Polyamide interfacial composite membranes prepared from m-phenylene diamine, trimesoyl chloride and a new disulfonated diamine. *J. Membr. Sci.*, 403-404, 152-161 (2012). <https://doi.org/10.1016/j.memsci.2012.02.038>
- Xu, J., Xu, Z., Poly(vinyl chloride) (PVC) hollow fiber ultrafiltration membranes prepared from PVC/additives/solvent. *J. Membr. Sci.*, 208 (1-2), 203-212 (2002). [https://doi.org/10.1016/S0376-7388\(02\)00261-2](https://doi.org/10.1016/S0376-7388(02)00261-2)
- Yan, W., Wang, Z., Wu, J., Zhao, S., Wang, J., Wang, S., Enhancing the flux of brackish water TFC RO membrane by improving support surface porosity via a secondary pore-forming method. *J. Membr. Sci.*, 498, 227-241 (2016). <https://doi.org/10.1016/j.memsci.2015.10.029>
- Yong, Z., Sanchuan, Y., Meihong, L., Congjie, G., Polyamide thin film composite membrane prepared from m-phenylenediamine and m-phenylenediamine-5-sulfonic acid. *J. Membr. Sci.*, 270 (1-2), 162-168 (2006). <https://doi.org/10.1016/j.memsci.2005.06.053>
- Yu, Z., Liu, X., Zhao, F., Liang, X., Tian, Y., Fabrication of a low-cost nano-SiO<sub>2</sub>/PVC composite ultrafiltration membrane and its antifouling performance. *J. Appl. Polym. Sci.*, 132 (2), 41267-41277 (2014). <https://doi.org/10.1002/app.41267>
- Yu, Z., Zhao, Y., Gao, B., Liu, X., Jia, L., Zhao, F., Ma, J., Performance of novel a Ag-n-TiO<sub>2</sub>/PVC reinforced hollow fiber membrane applied in water purification: in situ antibacterial properties and resistance to biofouling. *RSC Adv.*, 5 (118), 97320-97329 (2015). <https://doi.org/10.1039/C5RA18185B>
- Zhang, X., Chen, Y., Konsowa, A., Zhu, X., Crittenden, J., Evaluation of an innovative polyvinyl chloride (PVC) ultrafiltration membrane for wastewater treatment. *Sep. Purif. Technol.*, 70 (1), 71-78 (2009). <https://doi.org/10.1016/j.seppur.2009.08.019>
- Zhao, Y., Lu, J., Liu, X., Wang, Y., Lin, J., Peng, N., Li, J., Zhao, F., Performance enhancement of polyvinyl chloride ultrafiltration membrane modified with graphene oxide. *J. Colloid Interface Sci.*, 480, 1-8 (2016). <https://doi.org/10.1016/j.jcis.2016.06.075>